Comparison of CW-Lidar-Measured Wind Values Obtained by Full Conical Scan, Conical Sector Scan and Two-Point Techniques

R. L. SCHWIESOW,[1] F. KÖPP AND CH. WERNER

Institute for Optoelectronics, DFVLR Oberpfaffenhofen, D-8031 Wessling/Obb., Federal Republic of Germany

(Manuscript received 16 November 1983, in final form 5 October 1984)

ABSTRACT

Continuous-wave (CW) Doppler lidar measurements of wind magnitude and direction that are based on radial velocity data on only a *part* of a full azimuth circle compare favorably with measurements based on a *full* circle. Winds were measured over an altitude range of 750 m. For example, the rms difference between 76 wind data pairs at various altitudes, taken from a full circle and from a 1/4-circle sector is 0.43 m s^{-1} in magnitude (correlation coefficient 0.98) and 4.2° in direction, even when only 12 s of measurement time is used for the 1/4-circle sector. Increased integration time leads to an even closer comparison. Useful velocity estimates can be obtained from sector scans as small as 1/16 of a circle when a weighted least-squares fitting program is used to analyze the radial velocity versus azimuth data. Results from a two-point scan technique compare less favorably with the full-scan results than do results from a sector-scan technique. A scan employing a $\pi/2$, two-point azimuth difference results in an rms difference of 0.78 m s^{-1} (correlation coefficient 0.95) for 2 s of measurement time when compared with a full circle scan. We conclude that even if data are available or of interest over only part of an azimuth circle, good wind estimates are still possible.

1. The problem

Typical heterodyne Doppler lidars are remote sensing devices that measure the radial component of the wind, that is, the velocity component along the lidar line of sight. In order to infer the magnitude and direction of the horizontal wind, or to determine all three wind components with a single lidar, some form of scanning in azimuth is required. We used a continuous-wave (CW) lidar to obtain wind profiles to an altitude of 750 m, and we compare results obtained from different types of scans.

Lhermitte and Atlas (1961) showed that it is possible to derive mean horizontal wind magnitude and direction from radial velocity data taken from measurements arranged around horizontal circles centered on the vertical axis of the scanner. By varying the altitude of the circles, one can measure vertical profiles of the horizontal wind. This type of scan pattern is called a conical scan because the lidar beam sweeps out an inverted cone with the apex at the scanner. Because the data consist of radial velocity values as a function of scan azimuth, the pattern is also known as a velocity-azimuth-display (VAD) scan. Figure 1 shows cones swept out by VAD scans at different elevation angles and ranges. Scans corresponding to each different cone allow wind measurement on circles at different altitudes.

The goal of our study is to examine some representative VAD Doppler lidar data for internal consistency and to determine whether reasonable wind estimates can be made from data taken on only a sector of a VAD scan. The internal consistency of the data should be affected adversely by horizontal inhomogeneity in the wind field. By analyzing radial velocity data on part of a circle, we demonstrate the utility of fitting a segment of a sine wave to the measurements, using a least-squares method.

a. Horizontal inhomogeneity

Extracting three components of the wind from a single circular scan requires horizontal homogeneity in the wind field. Such homogeneity is often lacking, particularly in the presence of convective cells and similar perturbations, as has been demonstrated by lidar measurements of DiMarzio *et al.* (1979) and others. For example, DiMarzio *et al.* show differences of more than 16 m s^{-1} between radial velocities from regions separated by 30° in azimuth and approximately 2 km in distance. McCarthy *et al.* (1983) measured a number of surface divergence situations with radial velocity differences of 20 m s^{-1} or more over distances of approximately 2 km. Situations such as terrain changes and the presence of structures also lead to spatial inhomogeneities in the wind field.

Browning and Wexler (1968) have shown that the dominant effect in a VAD scan is from wind speed and direction, but that the zeroth Fourier component is proportional to divergence and the second-order term is proportional to pure deformation. For diver-

[1] Permanent affiliation: NOAA/ERL/WPL, Boulder, CO 80303.

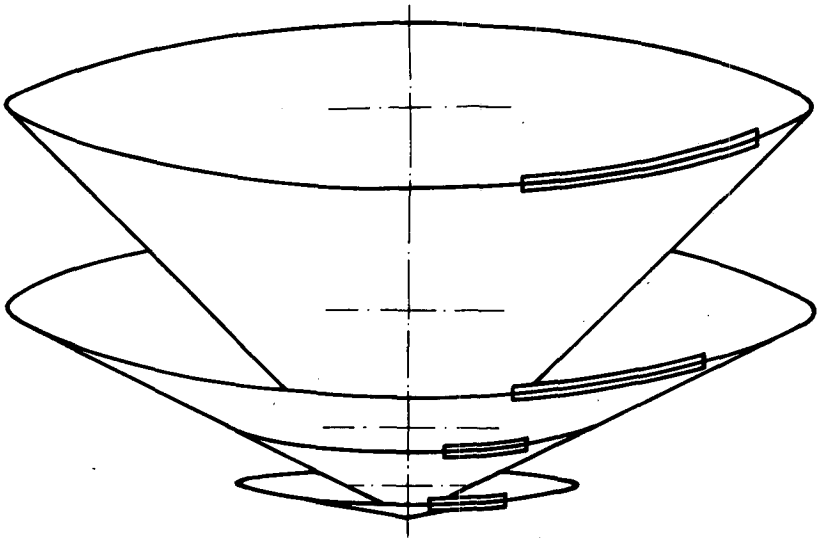

FIG. 1. Perspective view of conical scans at four altitudes, including two range settings and three elevation angles in various combinations. The part of the circle scanned by the lidar that is used for a typical ⅛-circle sector scan is drawn in triple lines.

gence and deformation to be detectable, the diameter of the circle on which the radial velocity component is measured must be large, because the contribution of the zeroth and second harmonics is proportional to range. Browning and Wexler calculate that the contribution of these terms is the order of 1 m s^{-1} for a range of 10 km. Because our range is less than 1 km, the effect of divergence and deformation should be more than an order of magnitude less than in the radar case and can be neglected. We consider only the first Fourier component for the lidar VAD analysis.

Because of the dominance of the first harmonic, our study addresses the effect of inhomogeneities (rather than linear variations) in the wind field on Doppler lidar measurements in the boundary layer. We compare wind vector inferences from actual data taken with various levels of inhomogeneity and temporal fluctuations. From differences in values inferred from different parts of the scan we can estimate uncertainties caused by inhomogeneity.

b. *Area restrictions*

In many applications of Doppler lidar, the lidar is not centered under the area of interest; measuring the wind vector along the approach path to a runway with a lidar near the touchdown point is one example. The scan pattern for a lidar is often blocked at some azimuths by buildings or other objects, so that only a part of the scanned circle provides useful data. For example, measurement of wind profiles close to the ocean surface with a downward-pointing lidar on an elevated platform must be done with a restricted scan pattern.

Because of these types of restrictions, we undertook to determine how representative of the overall wind values are wind values derived from scans over part of a horizontal circle. We were able to derive the horizontal wind from scans of ½, ¼, ⅛, and 1/16 of a full circle.

c. *Previous work*

Waldteufel and Corbin (1979) analyze the information available from conical scans taken in a wind field in which the magnitude of the components varies linearly with distance from a reference point. Easterbrook (1975) discusses a conical sector scan. Neither study is directly applicable to our lidar problem because both use data taken on a cone with varying range and azimuth, that is, with measurement points distributed over the surface of the sample cone rather than limited to a horizontal circle. Our lidar data were taken on a single circle because our interest is primarily in vertical profiles of the horizontal wind and because producing a data set on the entire surface of the cone with a CW Doppler lidar is too time-consuming to be practical, given the present data-processing capability of CW Doppler lidars.

In addition to the difference in data concentration between lidar measurements and the radar-derived data considered by Waldteufel and Corbin and by Easterbrook, the distance scale for their radars is more than an order of magnitude larger than that for our lidar. Thus, properties of the wind field such as convergence and deformation that are relevant in the case of a radar scan area of 20 × 20 km are not so relevant for a lidar scan area of 0.5 × 0.5 km. The

large scale of radar measurements also means that inferences about the influence of horizontal inhomogeneity on wind values measured with radar may not be valid when applied to the scale of short-range CW Doppler lidar.

Rabin and Zrnic' (1980) as well as Browning and Wexler (1968) discuss some of the possible errors in wind values derived from VAD radar scans. Their work provides backgrounds for our comparison between wind values derived from different parts of a VAD scan. Teoste and Capes (1978) show the result of a single VAD scan using a pulsed Doppler lidar, and Köpp *et al.* (1984) compare wind profiles derived from a Doppler lidar by using VAD scanning with profiles from balloon sondes. Doviak and Zrnic' (1984) derive error variances for least-squares estimates of wind from VAD data.

Clifford *et al.* (1980) make a theoretical analysis of the effects of fluctuations in the wind on wind measurements by a two-point lidar method, but they provide no lidar data. Our study deals with conical scan lidar geometry as well as two-point lidar geometry, and it concentrates on analysis of actual lidar measurements.

2. Experiment and analysis

a. Continuous-wave, infrared Doppler lidar

The lidar equipment that we used for wind measurements produces results that compare well with wind measurements made using other techniques (Köpp *et al.*, 1984). For example, the rms difference between the radial wind component as measured by the lidar and by a sonic anemometer is 0.12 m s^{-1} for 60 s averages. Because of previous comparisons with other instrumentation, we were able to analyze the results from different scan techniques by reference to lidar values alone.

For purposes of comparing the results from different scan patterns, the spatial averaging inherent in the lidar sensing region (without scanning) is relevant. The length of the volume along the line of sight ranges from approximately 40 m at the 200 m range to slightly less than 1000 m at the 1000 m range. This translates into an averaging interval in altitude ranging between 4 m for data taken at 20 m altitude to 760 m for data taken at 750 m altitude. Köpp *et al.* (1984) give further details on the system and its sensing volume.

The scattering targets for an infrared lidar are natural particulates in the atmospheric aerosol. Most of the effective scatterers are in the size range 1–3 μm radius (Post, 1978) because for smaller scatterers the return is too weak and for larger scatterers the number density is too small. The backscatter coefficient in the boundary layer is usually adequate for good return from the 1 km range (Schwiesow *et al.*, 1981).

b. Site

The wind measurements that we use to analyze the influence of scan geometry on the inference of horizontal wind were taken in a region of flat terrain on a topographic relief scale of 100 km horizontally. On a smaller scale of 1 km and less there are obstructions. The site is mostly flat meadow with grass approximately 20 cm high. Trees 12–15 m high surround the site at a distance of 500 m to the north and 1000 m to the south, and a line of trees extends northeast from the lidar starting 30 m away. A building 8 m high lies 200 m southwest of the lidar, and two low mounds less than 2 m high are to the southeast.

Overall, the site is simple terrain, but it is not flat and smooth in the strict, small-scale sense used in micrometeorological and boundary-layer research because of large roughness elements in the neighborhood of the lidar. The least disturbed region of the site is the northwest-to-northeast quadrant, so that analyses are made for sectors of the scan that are positioned over the field in that quadrant. At low elevation angles a range of 200 m was used to center the sample volume as far from trees as possible, but at higher elevation angles longer ranges were used to make measurements at higher altitudes.

c. Scanning and data recording

Figure 1 represents conical scans at different range and elevation-angle settings. The part of each circle drawn in triple lines shows a typical region for sector scans of approximately ⅛th of a full circle. The view for Fig. 1 is to the southwest.

Because of the extent of the lidar sampling volume along the line of sight, the data come not from a single circle but from an annulus on the cone. The region scanned is an annular ring, as shown from above in Fig. 2. A sector scan of ⅛ of a circle covers only the shaded portion of the ring, which is just over 10% of the volume of the atmosphere sampled in a full scan. The maximum dimension of the region for a ⅛-circle sector is less than 40% of the diameter of a full scan. It is reasonable therefore to expect that the sector scan is less influenced than the full conical one by atmospheric inhomogeneities on the scale of a few hundred meters to a few kilometers.

For some applications, the fact that the center of the sampling volume for a sector scan is offset from the lidar scanner is important. The nature of the offset is obvious from Fig. 2. It can be chosen by selecting suitable range and elevation angle values for a particular altitude.

The equation for VAD scanning is carefully analyzed elsewhere (e.g., Browning and Wexler, 1968; Easterbrook, 1975) and need not be derived here. Rather, we express the standard equation

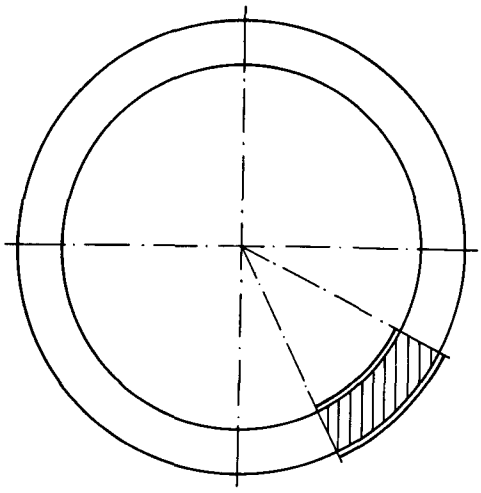

FIG. 2. Plan view of a conical scan showing the ring swept out by the lidar sample volume. The area involved in a ⅛-circle sector scan is shaded.

$$\mathbf{V}(\theta) = U\cos(\theta - \alpha)\cos\phi + w\sin\phi, \qquad (1)$$

where $\mathbf{V}$ is the measured radial component, U the horizontal wind speed, α its direction relative to $\theta = 0$, θ the azimuth of the scanner, ϕ the elevation angle, and w the vertical wind component in a form suitable for simple digital analysis. This form is

$$\mathbf{V} = |x(1)\cos\{s[i - x(2)]\} + x(3)| \qquad (1a)$$

in a homogeneous wind field. The data vector $\mathbf{V}$ is a 256-component array, and the wind variable x is a 3-component array, which is evaluated by a least-squares procedure. The azimuth is not considered a continuous variable, but takes on 256 discrete values $\theta = si$, where i takes on integer values from 0 to 255 and $s = 360/256$. Variable $x(1)$ is the magnitude of the horizontal velocity times the cosine of the elevation angle, $x(3)$ is the vertical velocity times the sine of the elevation angle, and $x(2)$ is the azimuth index (a number between 0 and 255) of the peak radial component. Variable $x(2)$ gives the direction of the wind. The independent variable is i. The absolute value is taken because the homodyne lidar system that we used could not determine the sign of the radial velocity.

An alternate form of (1) in more standard continuous form is

$$\mathbf{V} = |u\sin\theta\cos\phi + v\cos\theta\cos\phi + w\sin\phi| \qquad (1b)$$

(e.g., Easterbrook, 1975), where u and v are the horizontal wind components and θ is azimuth clockwise from the north (the independent variable). Although we used the nonlinear form (1) for convenience in comparing results from different sectors, it has no particular advantage over (1b). Least-squares fitting to (1b) for u, v, and w should be more efficient computationally than the nonlinear fit to (1), so (1b) will be used in future work.

In practice we scanned four full circles in approximately one minute and averaged the four scans to produce a single circular scan of 256 azimuth points. This procedure assured that our averaging interval was longer than a single scan so that temporal changes in the wind field during the scan would not appear as azimuth changes.

It is possible to simulate data from a two-point scan, which measures radial velocity at two different azimuths, by using part of the conical scan data. For this purpose we took five points that were located around each selected azimuth from the averaged scan. These five velocity values were averaged to give a single radial velocity value at each azimuth of the two-point scan. From the two values of radial velocity, $\mathbf{V}_1$ and $\mathbf{V}_2$, one can calculate by simple geometry the wind component across the bisector of the angle between the two measurement directions (cross wind) and the component along the bisector (longitudinal wind) as

$$|\mathbf{V}_c| = (\mathbf{V}_1 - \mathbf{V}_2)/(2\sin\alpha/2) \qquad (2)$$

$$|\mathbf{V}_l| = (\mathbf{V}_1 + \mathbf{V}_2)/(2\cos\alpha/2), \qquad (3)$$

where α is the angle between the two measurement directions. We calculated wind components for α values of $\pi/2$, $\pi/4$, and $\pi/8$ to correspond to sector scans of ¼, ⅛, and 1/16 of a full circle. With a homodyne system there is a fourfold ambiguity in $\mathbf{V}_c$ and $\mathbf{V}_l$ because the signs of $\mathbf{V}_1$ and $\mathbf{V}_2$ are unknown; therefore, for comparison purposes we chose those two-point component values that were closest to the cross-wind and longitudinal-wind values. These values were determined from the magnitude and direction of the wind inferred from the full conical scan.

Of course, representing the wind as components across and along a chosen direction is completely equivalent to a magnitude and direction representation. Cross-wind values are useful, for example, for aircraft operations such as runway approach and for computing ballistic aiming corrections. Special situations, in which surface conditions may influence the wind, or special areas, such as an approach path, which are of interest in the presence of possible convectively-induced spatial inhomogeneities in the wind field, may suggest a restricted sector size or a two-point scan angle smaller than 90°.

d. Least-squares fitting

One way to determine the three parameters $x(j)$ in (1a) from 256 data points is to use a least-squares fitting procedure. Because (1a) is nonlinear in $x(2)$, some sort of iterative procedure is useful (Schwiesow, 1982). With an iterative procedure, an initial guess from the raw data values leads to convergence of the fit in two to five iterations, depending on the closeness

of the guess to actual values and on the noisiness of the data. We are able to do the fitting with a fairly simple program in BASIC computer language.

The least-squares procedure allows us to weight data points. For the fitting, we removed all points with velocities below a threshold that included the minimum velocity that could be determined with our particular spectrum analysis system (Köpp *et al.*, 1984). This threshold was approximately 0.9 m s^{-1}, as is evident in the lower trace in Fig. 3. By eliminating velocity values that were below the threshold, we avoided distortions of the fit from data points that do not satisfy (1a) because they come from instrumental limitations rather than from atmospheric scatterers.

The standard deviation of the data points from the values computed from (1a) gives a measure of noise on the data or departures of the wind field from the horizontal homogeneity assumed in deriving the theoretical velocity versus azimuth expression. Thus the standard deviation of the fit tests the internal consistency of the data and gives a qualitative estimate of the uncertainty in the velocity estimate. We call this standard deviation a "fitting deviation" to distinguish it from the rms difference arising from the statistical comparison of wind estimates from different scan sizes.

3. Results

a. Illustrative examples

Particular cases illustrate a number of important aspects of the scan analysis program. The upper trace in Fig. 3 shows a typical low-noise VAD scan, which can be fitted with a small fitting deviation. Note that the trace should be approximately a *rectified* sine wave from (1a). This is why the data from four cycles of rotation show sharp "vees" near 0 m s^{-1}, where the sinewave changes sign, and rounded, sinusoidal peaks near 8 m s^{-1}. Fitting parameters are given in Table 1, where the first value for each sector size (*italics*) is that centered over the test field, and the second and third values are for sectors on either side of the center sector.

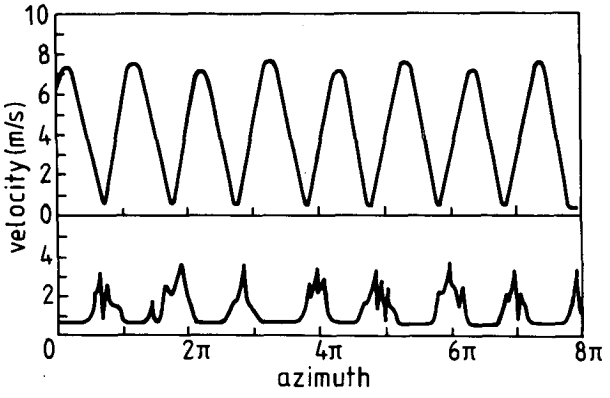

FIG. 3. Two examples of velocity-azimuth-display (VAD) data. The top scan represents low-noise data from a fairly homogeneous atmosphere, and the bottom is from a turbulent, inhomogeneous wind field. The traces are approximately four cycles of a rectified sinewave. The effect of the velocity threshold is especially noticeable in the lower trace. This threshold makes the weighted least-squares fitting desirable.

TABLE 1. Velocity estimates vs sector size for the upper trace in Fig. 3.

Sector size	Velocity (m s^{-1})	Azimuth (°)	Fitting deviation (m s^{-1})	Number of points
1/1	*11.9*	*153*	*0.09*	*233*
1/2	*11.5*	*153*	*0.16*	*119*
	12.4	154	0.12	116
1/4	*11.5*	*153*	*0.13*	*65*
	11.8	155	0.09	52
	12.0	151	0.15	55
1/8	*11.5*	*154*	*0.03*	*33*
	11.5	154	0.04	33
	12.1	151	0.16	31
1/16	*11.5*	*154*	*0.03*	*17*
	11.5	155	0.02	17
	11.7	153	0.03	17

The differences in velocity estimates between the different scan sizes are small (in every case < ±5%), and we attribute these differences to horizontal inhomogeneity in the wind field rather than to fitting uncertainties. The difference between velocity estimates from different sectors is ascribed to horizontal inhomogeneity because these differences between sectors are much larger than the fitting deviations within a sector, especially in the case of low-noise data. For example, in Table 1 the difference between upwind and downwind estimates for ½-circle sectors is 0.9 m s^{-1} but the fitting deviations are approximately ±0.15 m s^{-1}. Centers of the upwind and downwind sensing volumes are separated by approximately 400 m. Even in the case of noisy data from turbulent regions near the ground, for example the ¼-circle estimates from Table 2, the difference of sector estimates of 0.8 m s^{-1} is more than two fitting deviations. In this case the centers of the extreme sensing volumes were also approximately 400 m apart. These differences should not obscure the point that for low-noise data in this experiment the velocity differences from horizontal inhomogeneity are small fractions of the wind speed; the fitting deviations are smaller yet. Further support for this conclusion comes from values for $x(3)$, discussed later in the section.

In contrast to the low-noise scan, the lower trace in Fig. 3 represents a VAD scan in which turbulence causes relatively large fluctuations. In addition, the

TABLE 2. Velocity estimates vs sector size for the lower trace in Fig. 3.

Sector size	Velocity (m s^{-1})	Azimuth (°)	Fitting deviation (m s^{-1})	Number of points
1/1	*2.2*	*105*	*0.34*	*139*
1/2	*2.1*	*103*	*0.40*	*73*
	2.5	105	0.41	68
1/4	*2.1*	*105*	*0.34*	*21*
	1.9	113	0.32	41
	2.7	109	0.23	54
1/8	*1.7*	*116*	*0.14*	*5*
	1.9	119	0.37	33
	3.2	118	0.14	6
1/16	—	—	—	*1*
	2.2	113	0.17	13
	—	—	—	0

maximum radial velocity value is only two or three times the sensing threshold of the lidar system so that for some values of azimuth there are no velocity points from atmospheric scatterers. The fitting parameters for this worst case example (Table 2) behave similarly to those shown in Table 1 except that the fitting deviations are approximately three to five times larger and the velocity estimates for different sectors show a larger fractional variation.

The numbers of valid data points entering the fit are lower for the worst case scan than for the low-noise scan. In the extreme worst case sector (1/16-circle sector size and the radial component of the wind less than the system threshold) it is not possible to make a velocity estimate. Even for the 1/8-circle scan, some sectors have few data points and give velocity estimates that are not as close to the 1/1-circle velocity average as are estimates from sectors with more data points. For example, the third 1/8-circle sector in Table 2 has only six data points, so that the velocity estimate is unduly affected by the large turbulent fluctuations that can be seen in Fig. 3. This does not necessarily mean that such velocity estimates are in error, but simply that they are not as representative of the average wind field as are estimates coming from a larger number of data points. Of course, data from a small sector can be made more representative by time averaging for more than 48 s or four revolutions.

An inspection of Table 2 reveals that the number of data points entering the fit is a better criterion for the representativeness of the velocity estimate than is the standard deviation of the fit. In practice, therefore, we require that the number of valid data points in a sector be $\geq$40% of the maximum possible for a velocity estimate to be considered a representative value. This criterion was followed in producing the overall comparisons in the next section.

For both data samples in Fig. 3 the fitting procedure gives a value of -0.25 m s^{-1} for $x(3)$. Since the lower trace corresponds to an elevation angle of 5.7°, it is unreasonable to assume that $x(3)$ is a result of a vertical velocity of -2.5 m s^{-1} with a horizontal velocity of 2.2 m s^{-1}. Rather, in this case $x(3)$ must be a measure of horizontal inhomogeneity in the wind field. Divergence on a local scale is a special case of horizontal inhomogeneity and may affect the measurement, but we do not expect large-scale divergence to have a significant effect on our measurements (see Section 1a). For the upper trace in Fig. 3 it is possible, but unlikely under the stable atmospheric conditions prevailing at the time of the measurement, that the vertical velocity is -0.33 m s^{-1}. (The elevation angle for the upper trace was 49.5°.) These examples show the uncertainty in identifying $x(3)$ with vertical velocity in real, horizontally inhomogeneous boundary-layer flows on the scales studied in our experiment. Table 2 gives further evidence of the effect of horizontal inhomogeneity. In this case, for 1/2-circle sectors at 5.7° elevation the magnitudes of the upwind and downwind VAD peaks differ by 0.4 m s^{-1}, which is approximately twice $x(3)$, even in the case of near-horizontal measurements. Therefore, we do not report $x(3)$ as vertical velocity, and for sectors less than a full circle scan we do not fit $x(3)$ but hold it at 0 (for all elevation angles over the range 5.7 – 49.5°), so that the fitting procedure can operate with the fewest free parameters. This is consistent with the error analysis of Doviak and Zrnic' (1984), which shows that all three velocity components can not be estimated reliably from data on a small sector.

b. *Sector scan size*

To check the various wind estimates for internal consistency, we plotted the 1/2-circle estimates against a full scan and plotted estimates for 1/4-, 1/8- and 1/16-circle sectors against the estimate for the 1/2-circle sector that is centered over the test field. We compared the smaller sector results with the results from the 1/2-circle sector centered over the field rather than with the results from a full circle (1/1) because comparing results from a sector of 1/2-circle size reduced the effect of horizontal inhomogeneity. We considered only velocity values based on a number of data points at least 40% of the maximum possible number. Approximately equal numbers of scans centered at altitudes of 20, 50, 100, 200, 350 and 750 m enter the comparison. The data are not broken down by altitude for scan size comparison because we did not observe a significant difference between fitting results at different altitudes. Each scan can yield up to three comparison values for 1/4-, 1/8-, and 1/16-circle sectors because we considered the sector centered over the field and the two adjacent sectors, as shown in Tables 1 and 2.

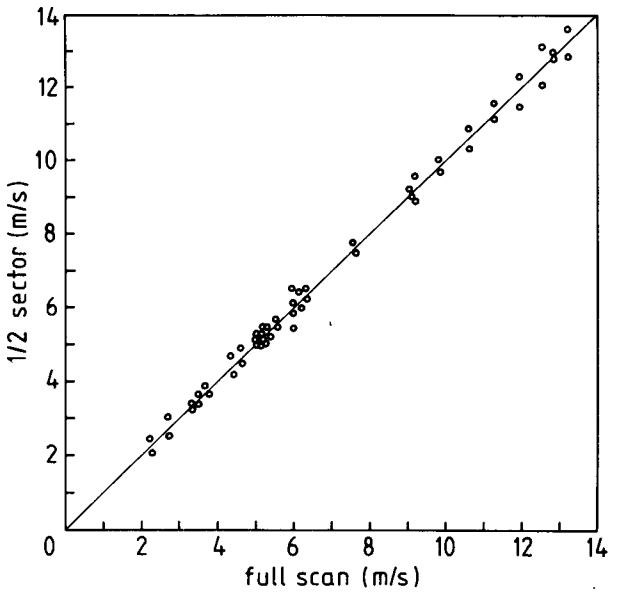

FIG. 4. Comparison of wind magnitude calculated from a ½-circle sector scan with that from a full scan (all data points considered). The diagonal line represents perfect identity between the two methods, not a fit to the comparison points. Statistical properties of the comparison plot are given in Table 3.

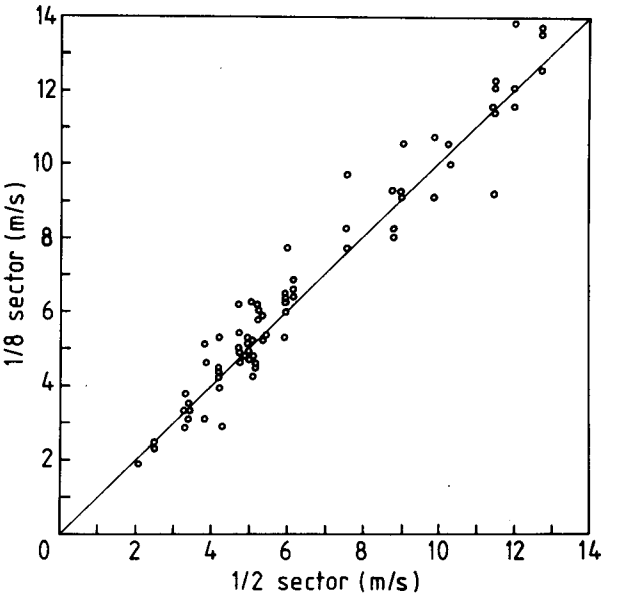

FIG. 6. As in Fig. 4 but for a ⅛-circle sector scan with an overlapping ½-circle sector scan.

The principal results for this part of the study are shown in Figs. 4–7, which compare the wind magnitude calculated from various sector sizes with the reference wind magnitude. Comparisons of wind direction estimates give similar scatter diagrams. Approximately 50 wind-estimate pairs enter the ½-circle versus 1/1-circle (full circle) comparison, and 75 pairs enter the other comparisons. It is clear that smaller sector sizes lead to more scatter in the wind estimate, as expected. Reasons for this scatter are analyzed in the next section.

Statistics of the wind-estimate comparisons shown in Figs. 4–7 are summarized in Table 3. The number of cases included in Table 3 are for ½ versus 1/1, 54; ¼ versus ½, 76; ⅛ versus ½, 73; and 1/16 versus ½,

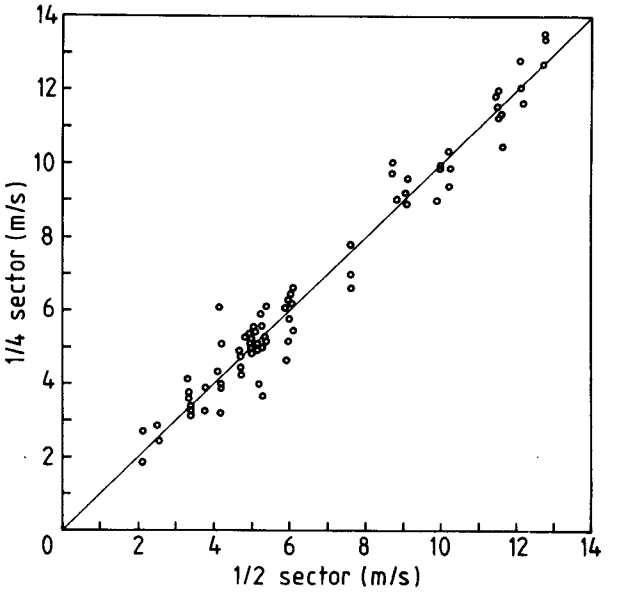

FIG. 5. As in Fig. 4 but for a ¼-circle sector scan with an overlapping ½-circle sector scan.

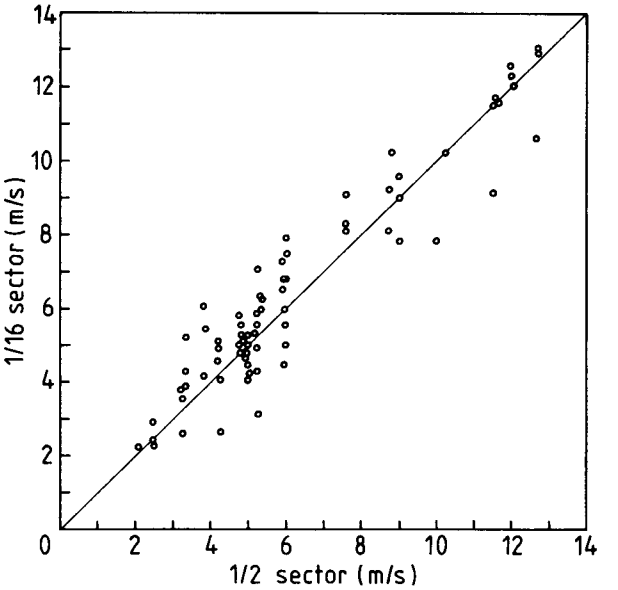

FIG. 7. As in Fig. 4 but for a 1/16-circle sector scan with an overlapping ½-circle sector scan.

TABLE 3. Statistical comparison of velocity estimates from various sector sizes (see Figs. 4–7).

	Magnitude		Direction	
Sectors	rms difference (m s^{-1})	Correlation	rms difference (°)	Correlation
1/2 vs 1/1	0.20	0.99	2.6	0.99
1/4 vs 1/2	0.43	0.98	4.2	0.97
1/8 vs 1/2	0.56	0.97	6.7	0.93
1/16 vs 1/2	0.71	0.94	11.6	0.80

71. The rms difference between 1/2-circle and 1/1-circle values for wind magnitude is similar in size to the rms differences in comparisons between different sensing methods (e.g., lidar and sonic anemometer by Köpp *et al.*, 1984), and it is less than 3% of the average wind magnitude in Fig. 4. The rms difference is also approximately the same as the average value of $x(3)$ for the 1/1-circle data, 0.19 m s^{-1}, so we conclude that the rms difference is a result of inhomogeneity in the wind field rather than of any inadequacy in using a 1/2-circle sector scan to estimate the horizontal wind. Noisy radial velocity estimates contribute to the fitting deviation in the analysis of each VAD sector. The resultant wind estimate for each sector may or may not be biased by the noise that results from atmospheric turbulence, depending on the distribution of radial velocity fluctuations with azimuth. Fluctuations that are sensed on an azimuth scale smaller than the sector size do not bias the final wind estimate. The rms difference between values of the wind direction that come from the two different sector sizes is less than 1% of a full circle, which is negligible for most applications.

Because we are dealing with statistical comparisons of results from a single lidar anemometer, it is not relevant to discuss experimental uncertainties in an absolute sense. The Doppler lidar anemometer is an inherently self-calibrated instrument because the conversion between measured frequency and the velocity of the scattering particles depends only on the laser wavelength and the speed of light. This results in negligible calibration error. The uncertainty of lidar wind measurements in comparison with other measurement techniques is analyzed by Post *et al.* (1978) and Köpp *et al.* (1984), among others. The rms differences and correlations in the tables of results are determined directly from the data set and have no uncertainty in themselves. The uncertainty in the results thus depends on the representativeness of the data set. This representativeness cannot be determined objectively but is best evaluated from the internal consistency of the data. We estimate a fractional uncertainty of approximately ±15% in the rms difference values.

In addition to velocity estimates that were rejected on the basis of the 40% (of maximum possible data points) criterion, 3 of 76 points for the 1/8-circle sector and 7 of 78 points for the 1/16-circle sector were rejected because their fitting deviations were more than three times larger than the average fitting deviation (see Fig. 8) for that sector size. Such obviously wild points are easy to detect and remove by an objective criterion based on fitting deviation.

c. *Temporal and spatial averaging*

The lidar data analysis system uses the peak of the received power spectrum to estimate the mean velocity in the sample volume. It is discussed more fully by Köpp *et al.* (1984). The system produces an average velocity estimate every 51 m s, and at an azimuth scan of 30° s^{-1} and 256 data points per revolution the dwell time per point is approximately 47 m s. Thus, the system makes one independent velocity estimate per data point. Four revolutions of a full-circle scan involve 48 s of data.

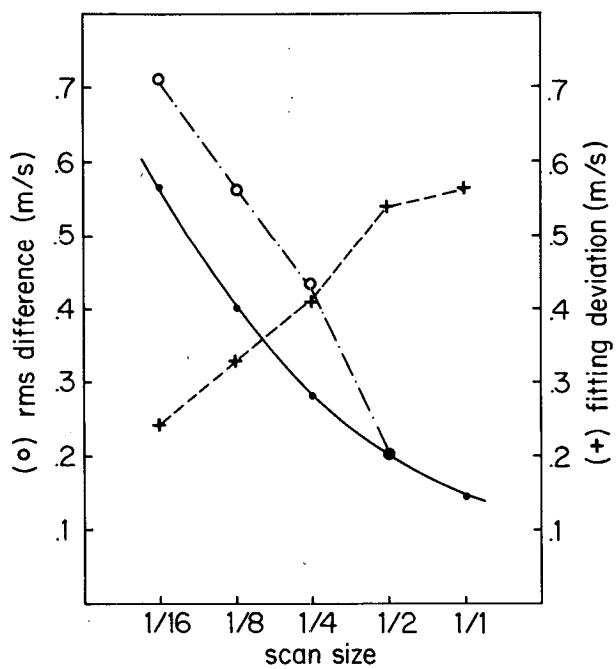

FIG. 8. Behavior of fitting deviation and rms difference as scan size changes. The fitting deviation (dashed connecting line) increases with the size of the sector scanned because the fit must include data from more widely separated parts of a more or less horizontally inhomogeneous atmosphere. The difference between a small-sector velocity estimate and the larger-sector average reference value (rms difference, dot-dashed connecting line) increases with decreasing sector size because the small-sector data are averaged over a small volume of the atmosphere and are therefore more responsive to spatial gradients. The solid line shows the statistically expected increase in rms difference that is proportional to $n^{-1/2}$, where n is the number of independent measurements leading to the velocity estimate.

Making a velocity estimate from only a sector of the scan or part of the data should result in a larger statistical uncertainty in the sector estimate than in the estimate from a full-circle scan. If we assume that there are many measurements and that all of the estimates are derived from the same statistical distribution, then the probable error of the sample mean estimate as a function of n independent measurements (or seconds) goes as $n^{-1/2}$, and we expect the statistical uncertainty (i.e., the rms difference between results from a sector and full-circle scan) to decrease also as $n^{-1/2}$. The rms differences in Table 3 show approximately this behavior. For example, a factor-of-4 increase in measurement time from a scan size of 1/16-circle to one of a 1/4-circle sector gives approximately a factor-of-2 decrease in the rms difference between estimates from a full circle and a part of a circle. A similar behavior holds for the change in rms difference between 1/8-circle and 1/2-circle sector scans. The rms differences for different sector sizes are shown graphically in Fig. 8. The fact that the rms differences are not exactly proportional to $n^{-1/2}$ shows that we do not have a large enough number of data pairs to give a precisely normal distribution and that the statistical distribution may not be stationary and may not be independent of azimuth.

We would expect the rms difference between a 1/16-circle sector scan and 1/1-circle scan, for example, to decrease with averaging time. Overall velocity averages in Table 4 support this expectation: for 71 data points the overall averages for 1/16-circle and 1/2-circle sectors differ by only 0.16 m s^{-1}, whereas the rms difference for single estimates is 0.71 m s^{-1}. However, we would not expect a factor of $71^{-1/2}$ $n^{-1/2}$) to apply to the overall average velocities compared to individual estimates because i) the wind field is not stationary; ii) differences in overall averages and rms differences are not the same quantity; iii) the rms difference between the 1/2-circle sector data and the full-circle data is itself greater than the difference in overall averages, so that there is some uncertainty in the reference average; and iv) effects, such as shadowing by the hedgerow, in addition to sample statistics can contribute to the difference in overall averages.

Although the rms difference of velocity estimates increases with decreasing sector size, the fitting deviation decreases with decreasing sector size. Consideration of spatial averaging explains this behavior, which is illustrated in Fig. 8. The smaller sectors include less effect from horizontal inhomogeneity and can therefore be fitted more accurately with (1a). Although the fitting is closer to the data points for a smaller sector compared with a larger sector, the resulting velocity estimate is generally less representative of the overall wind field, as illustrated by the comparisons in Table 3.

TABLE 4. Differences in overall average velocities from data in sectors of different sizes.

Sectors	Difference in magnitude (m s^{-1})/(%)	Difference in direction (°)
1/2 vs 1/1	+0.01/<1	−0.1
1/4 vs 1/2	0.00/<1	+0.6
1/8 vs 1/2	+0.21/3	+2.0
1/16 vs 1/2	+0.16/2	+3.6

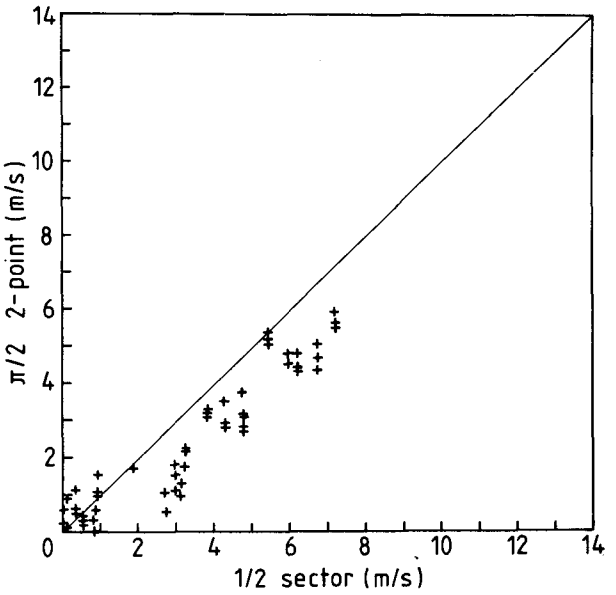

FIG. 9. Comparison of the cross-beam wind component calculated from two azimuth points 90° apart with that from an overlapping 1/2-circle sector scan. The diagonal line represents perfect identity between the two methods, not a fit to the comparison points. Statistical properties of the comparison are given in Table 5.

d. Two-point scan

The results of a comparison between the simulated two-point scan data and the 1/2-circle sector reference velocity estimates are shown in Figs. 9 through 11. The 1/2-circle rather than full-circle results are used as reference values because the 1/2-circle measurements and the two-point measurements were made in the same region. Even though the best two-point results were taken in cases of ambiguity, the two-point results are not as close to the reference values as are the sector scan results. Table 5 gives values for the rms differences between the two-point and reference velocity estimates. The low correlation coefficients in the case of $\pi/4$ and $\pi/8$ scan angles reflect the very wide scatter in Figs. 10 and 11; two-point and reference wind estimates are not well correlated.

For the simulated two-point data only 40 points or 1.9 s of data, which is only two-thirds of the data

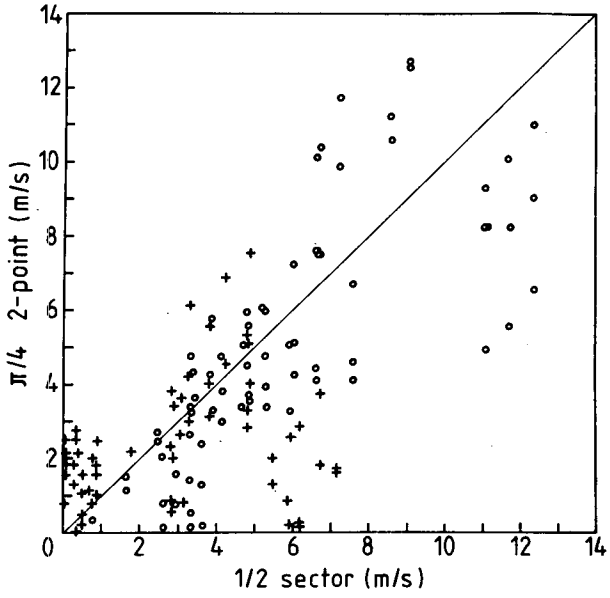

FIG. 10. Comparison of the cross-beam (crosses) and along-beam (circles) wind components calculated from two azimuth points 45° apart with those from an overlapping ½-circle sector scan. See also Table 5.

for a $\frac{1}{16}$-circle sector scan, were considered for each estimate. The ratio of the rms differences that result from two-point and $\frac{1}{16}$-circle sector scan comparisons with the $\frac{1}{2}$-circle reference should be $(1.9/3)^{-1/2} = 1.3$ if mean sample statistics are the controlling effect. Tables 3 and 5 show that the rms differences do not scale in the expected way with the number of independent velocity estimates in most cases. That

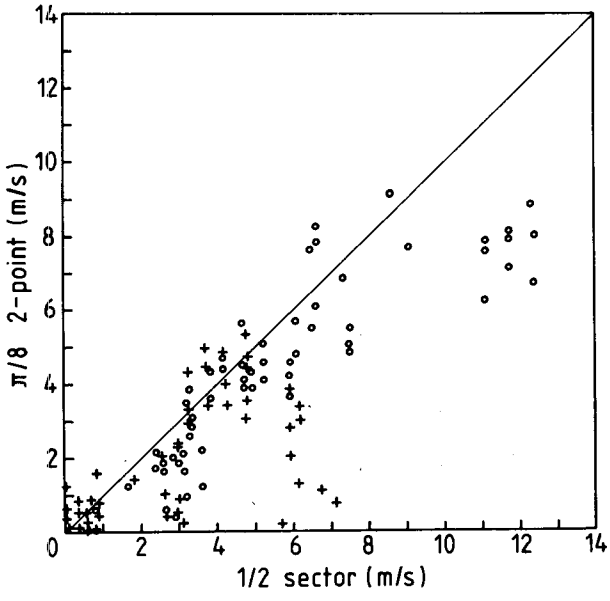

FIG. 11. As in Fig. 10 but points are 22.5° apart.

TABLE 5. Statistical comparison of two-point scan velocity estimates having different scan angles with a reference estimate from the $\frac{1}{2}$-circle sector scan.

	Cross component		Longitudinal component	
Δ azimuth	rms difference (m s^{-1})	Correlation	rms difference (m s^{-1})	Correlation
$\pi/2$	0.78	0.95	—	—
$\pi/4$	1.62	0.37	1.60	0.76
$\pi/8$	1.27	0.66	1.30	0.86
Average	1.22	—	1.45	—

is, the average rms differences in Table 5 are more than 30% larger than the expected 1.3 times the $\frac{1}{16}$-circle rms difference. The fact that the two-point and VAD measurements do not compare as $n^{-1/2}$ emphasizes that the assumption of a stationary statistical distribution is not completely valid for the measurements and that the two-point method is more sensitive to nonstationarity than is the VAD approach. The reason for the sensitivity involves both the comparative lack of spatial averaging in the two-point scan (discussed in the next paragraph) and the fact that the measurements at the two azimuths are not made simultaneously but are compared as if they were [see (2) and (3)]. In other words, errors in the velocity estimate caused by turbulence on the scale of the scan diameter are not completely random. The relative lack of data (i.e., integration time) does not completely explain the unfavorable comparison between the two techniques because even overall average values in Table 6 from 75 separate estimates are not close to reference values. It is instructive to compare Tables 6 and 4. Since the average values of wind components are generally smaller than the wind magnitude, the overall average differences in Table 6 compared with Table 4 are even worse than the absolute difference would indicate. The differences in overall averages are near 20–30% for the two-point scan and are an order of magnitude less for the sector scans. An additional conclusion from an assumption of a stationary statistical distribution is that the rms difference between two-point and reference results should be independent of the azimuth difference between the two points. Tables 3 and 5 show that the rms difference is not independent of the azimuth differ-

TABLE 6. Difference between overall average velocities determined from two-point scan data and those from the $\frac{1}{2}$-circle reference data.

Δ azimuth	Cross component difference (m s^{-1})/(%)	Longitudinal component difference (m s^{-1})/(%)
$\pi/2$	−0.71/36	—
$\pi/4$	−0.31/14	−0.68/14
$\pi/8$	−0.75/50	−1.07/25

ence, which is consistent with the nonstationary statistics inferred from the breakdown of $n^{-1/2}$ dependence.

There are two major reasons for the relatively poor performance of the two-point method compared with the sector scan: less efficient use of *a priori* knowledge of the variation of the radial wind with azimuth, and less spatial averaging. First, the least-squares fitting procedure utilizes the azimuth dependence in (1) to evaluate the relative contribution of each data point to magnitude and direction values. It is also easier to eliminate bad data points with the least-squares procedure then with two-point analysis. Second, the sector scan utilizes and averages data from the entire sector whereas the two-point scan uses data only from the edges of the sector. Thus the two-point wind estimates are more subject to errors arising from inhomogeneities in the wind field and turbulence on scales smaller than the sector size than are the sector scan estimates.

It is possible that longer data averaging for the two-point method would improve its performance. We do not have data available to check this hypothesis. The data reduction for (2) is simpler and faster than that for (1), a fact which gives the two-point scan a computational advantage over the sector scan. In practice, however, the alternating right-to-left, two-point scanning of a rather heavy mirror assembly is more difficult than the continuously rotating azimuth scan used for the sector results. Most of the time in taking real, rather than simulated, two-point data sets is spent in accelerating and decelerating the scanner rather than in measuring the wind.

4. Conclusions

The analyzed data show that good wind estimates are available from a CW Doppler lidar operating with a VAD scan over only part of an azimuth circle. Experimental situations in which surface features or convective cells may disrupt the spatial uniformity of the wind field over part of the region that is scanned can still permit use of a conically scanned Doppler lidar for wind profile measurements.

a. Scan method

For a given sector size, the sector scan method gives better results than the simulated two-point scan. Sector scan results for wind magnitude and direction compare very well (e.g., an rms difference of 0.20 m s^{-1} and 1.6°) with full conical scan results down to sectors as small as $1/16$ of a full circle if the VAD data are properly weighted to eliminate from consideration those measurements below a preset velocity threshold. For some combinations of wind direction, low wind magnitude and high instrumental threshold it is not possible to make a valid wind estimate with a $1/16$ sector scan. The rms differences between sector and full conical scans generally follow the predictions of sample mean statistics, so that data averaging can be used to reduce the rms differences between smaller sector scans and larger, but the rms differences do not exactly follow the $n^{-1/2}$ statistical predictions because the assumption of stationarity of the statistical distribution is not strictly true.

Smaller sector scans are less affected by inhomogeneities in the wind field on scales of the scan diameter than are full circle scans, as demonstrated by the dependence of fitting deviation on sector size. However, for the same number of scans the small-sector wind estimates are less representative of the overall wind field than are full scans because turbulent fluctuations on scales smaller than the scan diameter affect the small-sector values. Averaging times longer than the 48 s used in our experiment can make small-sector scans more representative of the wind field in a particular location; full scans average over small-scale turbulence.

A two-point scanning technique does not make as effective use of the radial wind information in a given sector as a sector scan does. This inefficiency is reflected in larger rms differences between results of the two-point method and those of reference ½-circle scans than between results of a small-sector scan and the same reference scan.

Details of a particular application and site determine the best sector size for making measurements of the horizontal wind. Our results show that the larger the sector the better the wind estimate for a fixed number of scans. However, increasing the number of scans for a sector to make the measurement time similar to the full-circle scan measurement time can result in measurements with a statistical uncertainty of ±0.2 m s^{-1} for a $1/16$-circle sector scan under typical boundary-layer conditions.

b. Other work

Clifford *et al.* (1980) considered theoretically a two-point scan and concluded that the scan angle should be at least 20° to obtain wind direction to ±10°. They did not consider averaging time, wind magnitude, or other types of scan. Our sector scan results for a 3 s measurement time and $1/16$-circle sector (22.5°) show a standard deviation of 11.6° and so are consistent with the expectations of Clifford *et al.*

We are not aware of other sector scan lidar measurements with which our work can be compared. The validity of full conical scan lidar measurements of horizontal wind profiles in the boundary layer has been established by Köpp *et al.* (1984).

c. Further research

Based on our experience, we conclude that the least-squares fitting program used to evaluate the data

by (1) for wind magnitude and direction can be made considerably faster than the version used in this experiment. Further studies of small-sector scans (e.g., $\frac{1}{8}$ and $\frac{1}{16}$ of a circle) with longer averaging time would be worthwhile to confirm the representativeness of wind estimates that result from small-sector scans in the boundary layer.

It would be interesting to compare wind estimates made from direct, time-of-flight measurements (i.e., the time for a scattering center to pass between two closely spaced lidar beams) of the wind transverse to the lidar axis (e.g., Lading *et al.*, 1978) and Doppler lidar measurements of the along-axis component with conical-sector-scan estimates of wind magnitude and direction, because these different methods have significantly different volume-averaging characteristics and respond to the various scales of atmospheric fluctuations in different ways.

Acknowledgments. H. Herrmann developed the scanner, which was essential to the work, and F. Bachstein was in charge of the data system. M. Klier supported the practical aspects of the field experiment and U. Manenstein prepared the figures.

REFERENCES

Browning, K. A., and R. Wexler, 1968: The determination of kinematic properties of a wind field using Doppler radar. *J. Appl. Meteor.*, **7**, 105–113.

Clifford, S. F., T. R. Lawrence, G. R. Ochs and T-i. Wang, 1980: Study of a pulsed coherent lidar for crosswind sensing. NOAA Tech. Memo. ERL WPL-48, NOAA/ERL, Boulder, CO, 47 pp.

DiMarzio, C., C. Harris, J. W. Bilbro, E. A. Weaver, D. C. Burnham and J. N. Hallock, 1979: Pulsed laser Doppler measurements of wind shear. *Bull. Amer. Meteor. Soc.*, **60**, 1061–1066.

Doviak, R. J., and D. S. Zrnic', 1984: *Doppler Radar and Weather Observations*, Academic Press, 458 pp.

Easterbrook, C. C., 1975: Estimating horizontal wind fields by two-dimensional curve fitting of single Doppler radar measurements. *Preprints, Sixteenth Radar Meteorology Conf.*, Houston, Amer. Meteor. Soc., 214–219.

Köpp, F., R. L. Schwiesow and Ch. Werner, 1984: Remote measurements of boundary-layer wind profiles using a CW Doppler lidar. *J. Climate Appl. Meteor.*, **23**, 148–154.

Lading, L., A. Skov Jensen, C. Fog and H. Andersen, 1978: Time-of-flight laser anemometer for velocity measurements in the atmosphere. *Appl. Opt.*, **17**, 1486–1488.

Lhermitte, R. M., and D. Atlas, 1961: Precipitation motion by pulse Doppler. *Preprints, Ninth Weather Radar Conf.*, Kansas City, Amer. Meteor. Soc., 218–223.

McCarthy, J., R. Roberts and W. Schreiber, 1983: JAWS data collection, analysis highlights, and microburst statistics. *Preprints, 21st Conf. on Radar Meteorology*, Edmonton, Amer. Meteor. Soc., 596–601.

Post, M. J., 1978: Experimental measurements of atmospheric aerosol inhomogeneities. *Opt. Lett.*, **2**, 166–168.

——, R. L. Schwiesow, R. E. Cupp, D. A. Haugen and J. T. Newman, 1978: A comparison of anemometer- and lidar-sensed wind velocity data. *J. Appl. Meteor.*, **17**, 1179–1181.

Rabin, R., and D. Zrnic', 1980: Subsynoptic-scale vertical wind revealed by dual Doppler-radar and VAD analysis. *J. Atmos. Sci.*, **37**, 644–654.

Schwiesow, R. L., 1982: Nonlinear least squares fitting on a minicomputer: Method and example. NOAA Tech. Report ERL 421-WPL 57, NOAA/ERL, Boulder, CO, 12 pp.

——, R. E. Cupp, V. E. Derr, E. W. Barrett and R. F. Pueschel, 1981: Aerosol backscatter coefficient profiles measured at 10.6 μm. *J. Appl. Meteor.*, **20**, 184–194.

Teoste, R., and R. N. Capes, 1978: High-altitude infrared radar wind measurements. *J. Appl. Meteor.*, **17**, 1575–1578.

Waldteufel, P., and H. Corbin, 1979: On the analysis of single-Doppler radar data. *J. Appl. Meteor.*, **18**, 532–542.